What M dwarf models reveal about their UV spectra?

Dennis Tilipman[1,2], Mariela Vieytes[3,4], and Jeffrey L. Linsky[2,5]

1. National Solar Observatory, Boulder, CO 80309
2. Department of Astrophysical and Planetary Sciences, University of Colorado, Boulder, CO 80309
3. Instituto de Astronomía y Física del Espacio (UBA-CONICET), Buenos Aires, Argentina
4. National University of Tres de Febrero, 2736, AHF, Av. Gral. Mosconi, B1674 Senz Pea, Buenos Aires, Argentina
5. JILA, University of Colorado, Boulder, CO 80309

Abstract

Stellar ultraviolet (UV) radiation has significant implications on habitability of their exoplanets, yet this radiation is partly unobservable due to interstellar medium absorption. We used the radiative transfer code SSRPM to build stellar models of two M dwarfs and synthesize their UV spectra, particularly focusing on the far-UV and extreme-UV spectra. Our most important findings are that 1) the coronae of two M dwarfs are responsible for more than half of their respective EUV fluxes, and 2) the continuum in the FUV band between 145 and 170 nm is responsible for about half of total emission in this band. Here, we discuss the significance of these results and outline future projects aimed to improve our understanding of solar and stellar UV emission.

Motivation and Methods

M dwarfs are hosts to the majority of known exoplanets. However, the photochemical processes occurring on these exoplanets are somewhat unknown, since they are determined in large part by the ultraviolet (UV) radiation environment created by their host stars. This UV radiation is often unobservable due to 1) intrinsic faintness of M dwarfs and 2) absorption by interstellar medium. Such is the case especially for the extreme-UV (EUV, 100–912 Å) spectra and far-UV (FUV) continua. In our recently accepted paper (Tilipman et al., 2020), we use a semi-empirical radiative transfer code SSRPM (Fontenla et al., 2016, and references within), which computes emerging spectra by solving simultaneously statistical equilibrium and radiative transfer equations for a one-dimensional model atmosphere. SSRPM is equipped with NLTE (non- local thermodynamic equilibrium) and PRD (partial redistribution) capabilities.

Model Validation

For our project, we picked two exoplanet hosting M dwarfs, GJ 832 and GJ 581. Their parameters are listed in Table 1. In order to synthesize reliable EUV spectra, which are unobservable, we built and iteratively improved the one-dimensional atmosphere models of these stars until synthetic spectra matched observed spectra where the latter were available. We used visible spectra observed with the CASLEO telescope in Argentine, and X-ray spectra from the publicly available MUSCLES Treasury Survey archive. Table 2 lists several key spectral features that were used for validation of the atmosphere models.

Table 1. Stellar Parameters

	GJ 832	GJ 581
d (pc)	4.965 ± 0.001	6.30 ± 0.01
R_* ($R_\odot$)	0.499 ± 0.017	0.299 ± 0.010
log [Fe/H]	0.06 ± 0.04	-0.33 ± 0.12
log g (cgs)	4.7	4.92 ± 0.10
Spectral type	M2	M3
$T_{\rm eff}$ (K)	3590 ± 100	3498 ± 56
Age (Gyr)	8.4	4.1 ± 0.3

Table 2. Average disk intensities (erg cm^{-2}Å^{-1}s^{-1}sr^{-1}) of key spectral lines

Feature & λ (Å)	GJ 832 synthetic	GJ 832 observed	error[a] (%)	GJ 581 synthetic	GJ 581 observed	error (%)
Ca II H & K 3950	1.13E4	1.23E4	8.13	5.21E3	...	...
Mg II h & k 2800	2.73E4	2.17E4[b]	25.8	6.83E3	7.19E3[b]	5.01
C II 1334	84.3	133[b]	36.8	43.9	62.2[b]	29.4
C II 1336	132	180	26.7	70.5	129	45.3
Si IV 1394	125	137	8.09	52.6	76.5	31.2
Si IV 1402	65.8	73.4	10.4	27.4	29.6	7.43
C IV 1548	201	323	37.8	325	297	9.43
C IV 1551	102	154	33.8	163	148	10.1
O IV 1401	7.92	11.6	31.7	2.38	7.37	67.7
N V 1239	121	138	12.3	138	90.5	52.5
N V 1243	60.2	67.1	10.3	69.2	50.2	37.8
Fe XII 1242	8.78	5.92	48.3	...	...	...
H I (Lyα) 1215.6	1.27E5	5.88E4[c]	116	8.89E4	3.18E4[c]	180

[a] Error is defined as percentage fractional difference, $\frac{|I_{observed} - I_{synthetic}|}{I_{observed}} \cdot 100\%$. This fractional difference exceeds measurement uncertainty in all cases except Si IV and C IV in GJ 581 spectra, where they are roughly equal (Youngblood et al. 2016)
[b] Observed fluxes were increased by 30% to account for interstellar absorption.
[c] Reconstructed Lyα flux from the MUSCLES portal

As can be seen on Figure 1, the atmospheric structures of GJ 832 and GJ 581 are fairly similar. This is to be expected, as they are of similar spectral types (see Table 1).
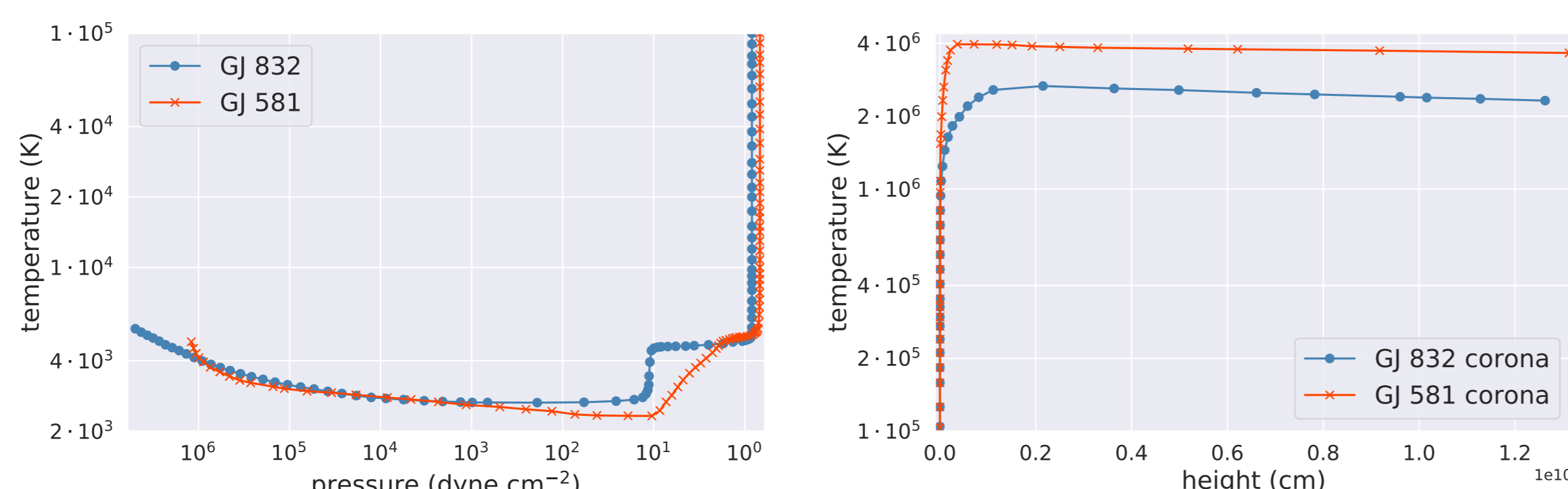

Figure 1: Thermal structures of GJ 832 (blue) and GJ 581 (orange). The figure on the left spans the photosphere, chromosphere, and lower transition region (TR), whereas the right panel shows the upper TR and corona (note the different x-axis units). The division between the lower and upper component models is significant, as we compute the two components separately and then match the boundary conditions. The differences are most prominent in the chromosphere and TR: the pressure at which the TR occurs is higher in GJ 832 compared to GJ 581, and the TR itself is steeper (not visible in this image). This indicates higher levels of chromospheric magnetic activity in GJ 832, which is consistent with higher fluxes of many UV lines that scale with magnetism (see Table 2).
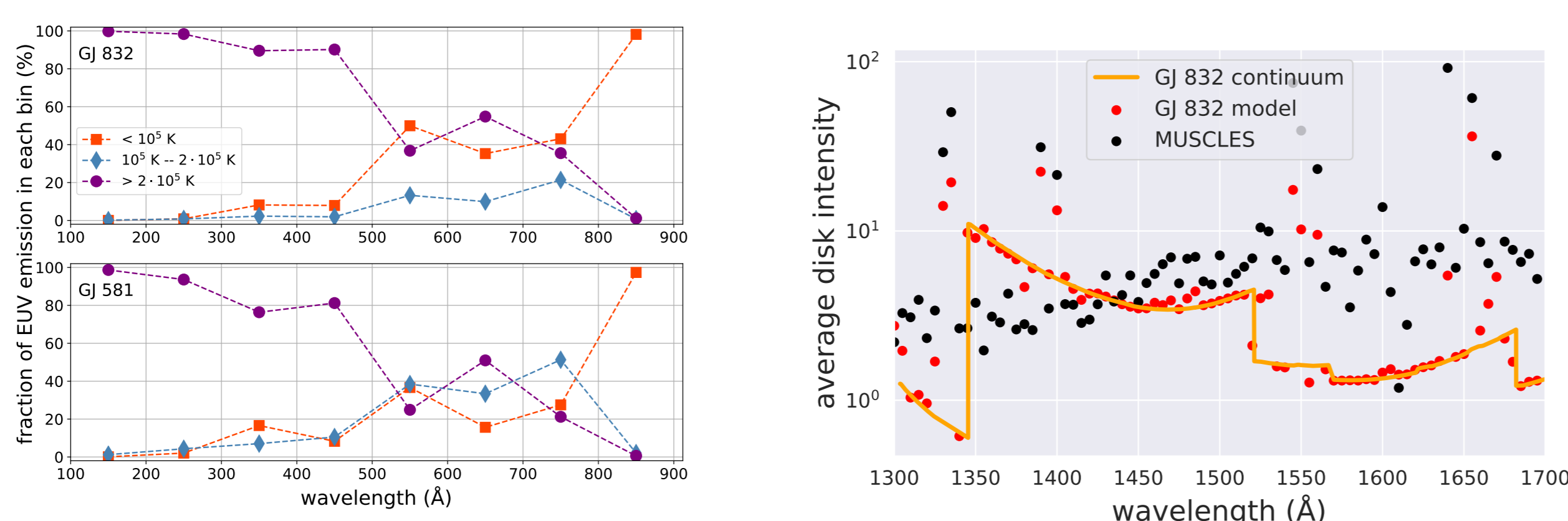
Main Results

Figure 2: *Left:* Fractional EUV emission in 100 Å bins for GJ 832 (top) and GJ 581 (bottom). The general trends are similar in two stars and make physical sense: EUV radiation of shorter wavelengths (< 500 Å) forms primarily in the hotter corona, while the cooler chromosphere and TR are responsible for longer wavelengths. *Right:* Synthetic and observed spectra of GJ 832 between 1300 Å and 1700 Å. Both are downsampled to 5 Å bins. Here we also show that our model incorrectly predicts a strong continuum edge at 1350 Å.

- We synthesized high-resolution ($R = 100,000$) EUV spectra of GJ 832 and GJ 581. We computed EUV contributions separately for three model components: the lower component includes all of the atmosphere below 100,000 K (corresponding to the photosphere, chromosphere, and lower TR), the middle component from 100,000 K to 200,000 K (TR), and the upper component above 200,000 K (corona). Particularly important is that coronal EUV emission accounts for more than half of total EUV emission of each star (Figure 2).

- The mostly unobservable FUV continuum between 1450 Å and 1700 Å contributes more than half of the emission in this band (Figure 2). This is noteworthy, as this radiation may affect oxygen photochemistry in exoplanet atmosphere.

- We synthesized panchromatic spectra of GJ 832 and GJ 581 (Figure 3). These spectra can be used as inputs for exoplanet studies.
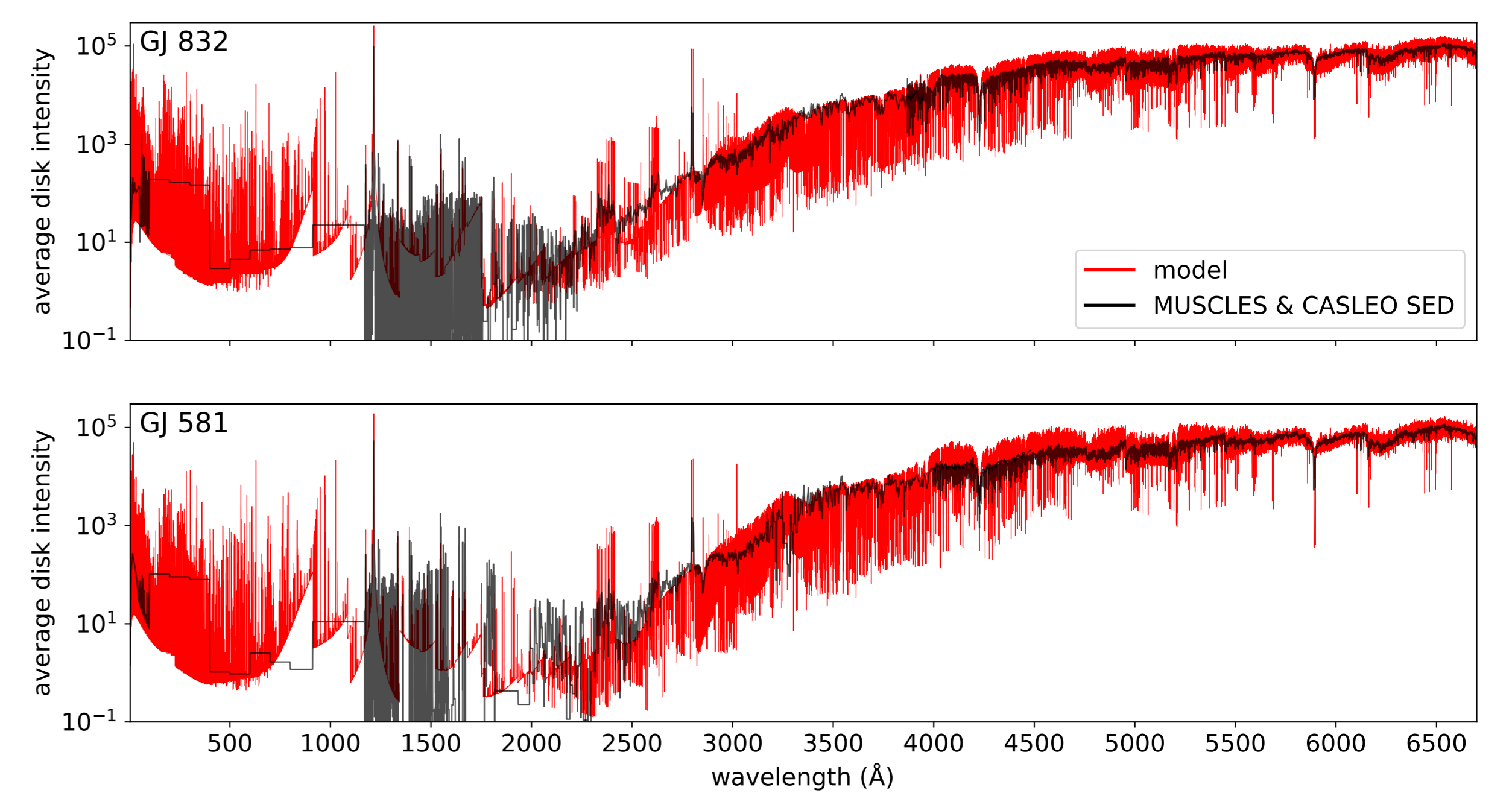

Figure 3: Panchromatic spectra of GJ 832 (top) and GJ 581 (bottom). Synthetic SSRPM spectra are shown in red, observed and reconstructed spectra are in black. The SSRPM spectra are shown in native SSRPM resolution, which exceeds resolution of MUSCLES and CASLEO spectra; hence the differences in emission and absorption line profiles are exaggerated on this image.

Ongoing work

We are currently investigating the origin of EUV emission in more detail. Instead of dividing the model atmospheres into two or three components, we are planning to divide them into at least five and see which of them contribute to EUV emission the most. We will also include existing solar models in this project to characterize any important differences between EUV emission of the sun and that of a M dwarf. In Figure 4, we show the contribution functions for several EUV wavelengths in the model atmosphere of GJ 581.
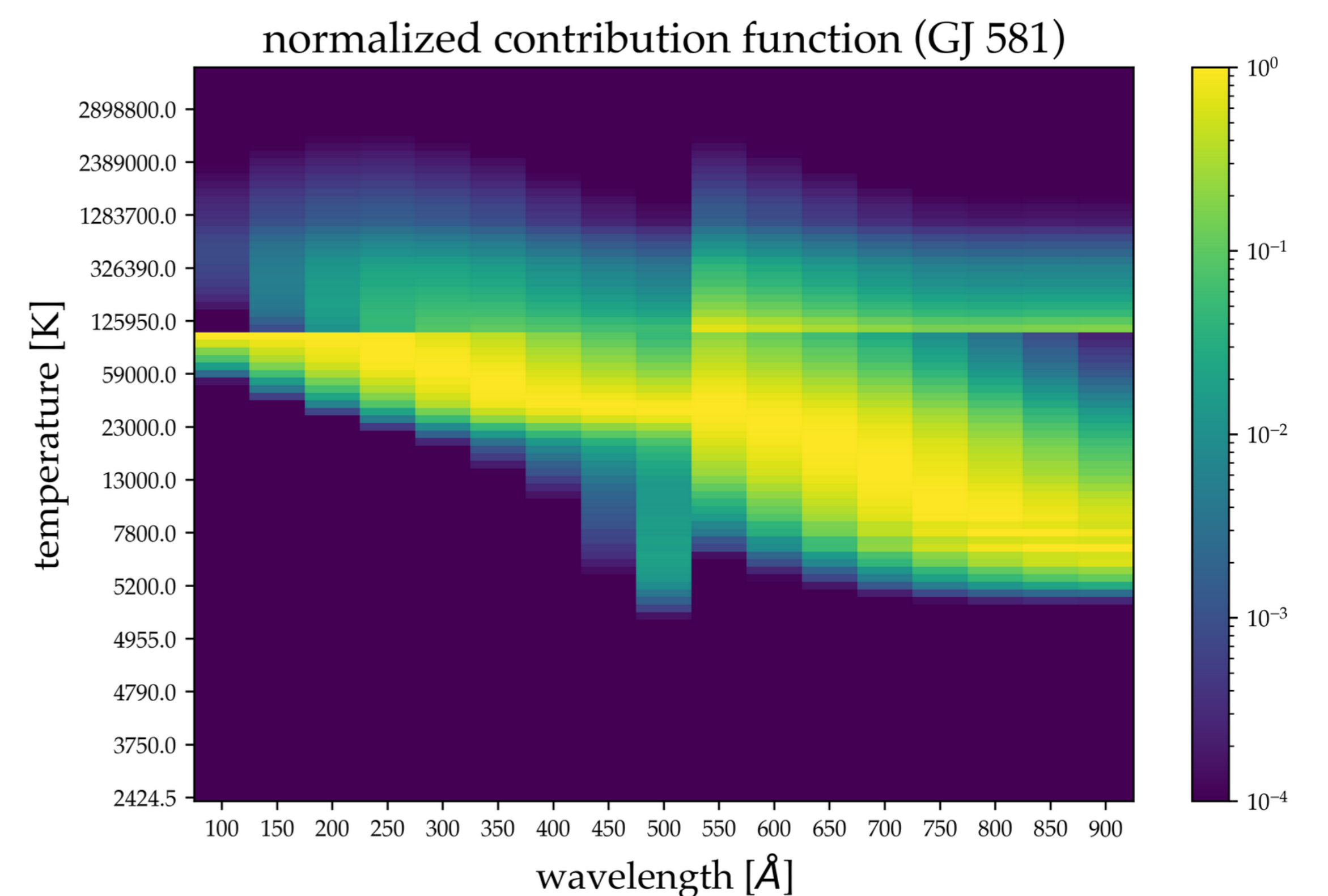

Figure 4: Normalized contribution functions in EUV wavelengths of GJ 581. The discontinuity at 100,000 K is due to the model atmosphere consisting of two components, and shows that there are some limitations to using the contribution function. However, it does provide us with a good sense of which heights are most important for EUV formation.

Links and contact info: Panchromatic synthetic spectra will be available for download at https://doi.org/10.17909/T9DG6F; currently available by request at dennis.tilipman@colorado.edu
SSRPM code and databases are available by request
Zoom ID for discussion: 358 741 3592; 22:00 − 23:00 UTC March 2-4; Passcode: CS205EUV

References

Fontenla, J. M., Linsky, J. L., Witbrod, J., et al. 2016, ApJ, 830, 154.

Tilipman, D., Vieytes, M., Linsky, J. L., et al. 2020, arXiv:2012.11738

Youngblood, A., France, K., Loyd, R. O. P., et al. 2016, ApJ, 824, 101